Hydrogen plasma induced by extreme ultra-violet radiation and its interaction with optical components in nanolithography research

A. Ushakov[1], J. van Veldhoven[1], C.-C. Wu[1], M. van Putten[1]

[1] *TNO The Netherlands Organization for Applied Scientific Research, Delft, The Netherlands*

Abstract: Low-density hydrogen plasma induced with a 13.5-nm Extreme Ultra-Violet (EUV) beam through photoionization is studied at pressures 2-20 Pa as it interacts with nanolithography photomasks in the test environment of the EBL-2 research facility. Changes of surface properties of Ru-capping layer correlate with plasma ion fluxes in space- and pressure-resolved tests. To achieve dose-dependent effects, increased pressures are considered for accelerated tests of materials in relevant nanolithography environments.

Keywords: EUV-induced plasma, photomask, nanolithography, reticle, surface oxidation

1. Introduction

In nanolithography machines, Extreme Ultraviolet (EUV) photons with wavelengths of 13.5 nm produce a low-density plasma due to photoionization of the hydrogen background gas typically used in the EUV beam delivery system [1,2]. The hydrogen plasma assists in etching possible carbon and tin contamination. Plasma induced by an EUV beam has been studied mainly in hydrogen and argon, to understand the long-term impact on delicate optics of nano-lithography scanners [1].

Ions, radicals, and electrons emitted from the plasma may influence the lifetime and the performance of contact-sensitive components of the lithography optics such as multi-layer mirrors, photomasks and pellicles. The EUV-induced plasma may affect materials in many ways such as blistering, roughening and chemical interactions [2,3]. In our earlier publications, characteristics of ion fluxes impinging on materials in EUV-induced plasmas were determined during the pulse afterglow [4].

EUV-induced plasmas are pulsed with a relatively low-density transient period between the pulses, where the plasma density can be estimated as 10^{13}-10^{14} m^{-3} and the electron temperature decays from 2-3 eV to a fraction of an electron-volt in tens of microseconds [5]. The pulse repetition rate in a modern EUV machine reaches tens of kilohertz [6]. Characteristic times of transient processes between two consecutive pulses may vary between 100 ns and tens of microseconds [1,2]. That complicates measurements to assess plasma density and temperature.

This complex low-density plasma environment requires further data build-up and process description and would be of interest for the research community focused on EUV optics, pellicles, and photomasks studies. Due to high operation costs and risks of contamination it is difficult to carry out experiments in a commercial EUV lithography system. Therefore, alternatives are considered [7].

A candidate technology for tests in an EUV environment including EUV-induced plasma is EBL2 – a research and testing 13.5-nm-beamline system commissioned at TNO [8-10]. It assists in developing nanolithography components and provides accelerated lifetime tests of mirrors and photomasks for next generation nanolithography in a controlled environment. In this paper, we continue studies of ion fluxes in EUV-induced plasmas and investigate the plasma interaction with EUV photomasks as they play a key role in the realization of high-volume manufacturing of integrated circuits on wafers.

2. Experimental setup

The method to produce EUV-induced plasma in the beam line of the EBL2 was discussed in [4]; the test configuration is briefly summarized in Fig. 1. The main components include: a high brightness EUV source operating in a repetitively pulsed mode at 3 kHz and 4.2 W EUV beam power, the collector chamber with mirrors M1 and M2 and the test chamber. A spectral purity filter (SPF) that removes the out-of-band spectrum (> 20 nm) can be installed in the intermediate focus of the beam (IF) between M1 and M2. The test chamber includes a moveable sample holder placed perpendicularly to the beam axis. The gas environments of the test chamber and the collector chamber are separated by an orifice and by using differential pumping.

The beam can be focused on the sample holder and projected onto the sample in a hydrogen gas in the pressure range of 1-20 Pa. The plasma is formed in the volume between sample and entrance of the light into the inner geometry of the test chamber as schematically presented in Fig. 2. The ion energies and fluxes of the plasma were measured using a compact retarding field (ion) energy analyzer (RFEA), perpendicular to the beam. A moveable sample holder could accurately position the RFEA with an accuracy of ± 0.1 mm (Fig. 2-b).

The RFEA could move in horizontal and vertical directions perpendicular to the EUV beam. The RFEA version was developed by Impedans Ltd. for low-energy ion fluxes such as $\Phi=10^{16}$-10^{19} ions·$m^{-2}s^{-1}$. Experimental parameters and general characteristics of the plasma measured in the experiments are summarized in Table 1. The current research is focused on measurements of ion fluxes from plasma. Hydrogen plasma produced due to the photoionization of the background gas creates intense fluxes of hydrogen radicals as well. Such radical fluxes may influence the performance of the sensitive optical equipment as they etch carbon and reduce the amount of oxidized materials [11].

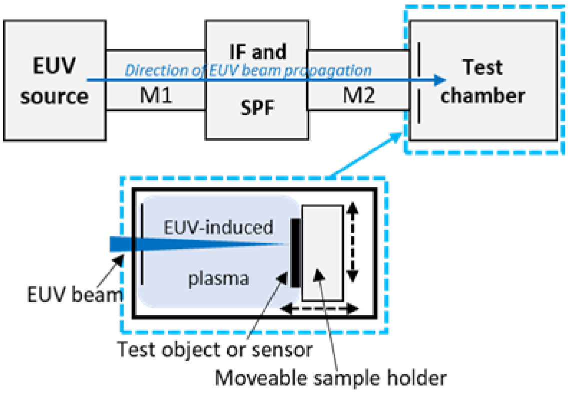

Fig. 1. The EBL-2 research facility overview.

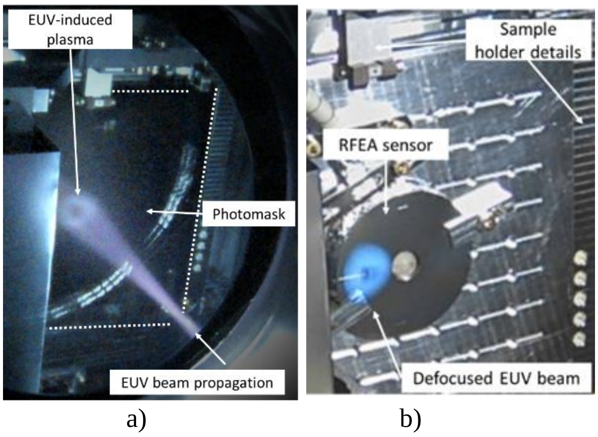

Fig. 2. Test configuration details: a) photo in visible light through the transparent vacuum window featuring EUV-induced plasma cone in the test chamber impinging on the photomask (white dotted lines show the borders of the photomask); b) RFEA sensor head with a partially defocused EUV beam spot next to it. The sensor head diameter is 50 mm.

However, methods for accurate measurements of such fluxes are yet to be defined. Attempts to develop a catalytic radical sensor based on the measurement of the heat release when radicals recombine on a surface show promising results [12] as an atomic hydrogen recombination rate with a linear response in the range of 10^{18}-10^{21} (atoms·$m^{-2}s^{-1}$) could be measured for plasma radical fluxes.

Table 1. EBL2 plasma measurements parameter space

Gas	Hydrogen
Operating pressures (Pa)	2-20
Test chamber background pressure (Pa)	$2 \cdot 10^{-6}$
Energy in one EUV pulse (J)	4.2
Pulse repetition rate (kHz)	3
Number of pulses per exposure ($\cdot 10^6$)	100-200
EUV peak intensity (mW/mm^2)	20-23
Ion energies (eV)	1-8
Highest ion flux (ions·$m^{-2}s^{-1}$)	10^{19}
Lowest ion flux at decay (ions·$m^{-2}s^{-1}$)	$(1\text{-}2) \cdot 10^{16}$

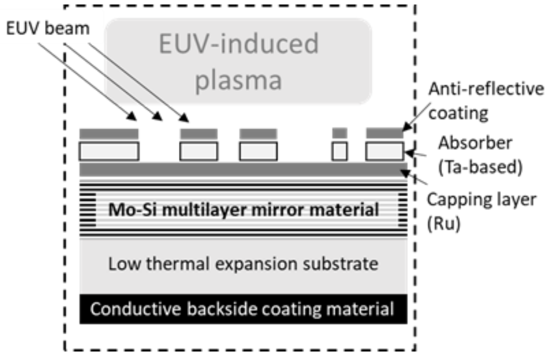

Fig. 3. Schematic representation of a photomask used in EUV-induced plasma tests.

A generic structure of a photomask as it is used to study interactions with the EUV beam and the plasma in our experiments is illustrated in Fig. 3. Here, we consider the contact of the absorber and capping layer of the photomask with the EUV induced plasma, which may contain contamination or results in the change of properties that influence the photomasks' optical performance.

3. Measurements of ion fluxes

Ions in the plasma are produced due to photoionization including the processes of single and double photoionization and of dissociative photoionization and then due to the electron impact ionization. The detailed process of the plasma formation was considered in [6]. For photons with an energy of 92 eV, most of the ionization events go via the reaction $g+H_2 \rightarrow e^- + H_2^+$. The photoionization process is complete within 1 µs and subsequent hydrogen ionization goes via electron impact ionization forming secondary electrons, with the major ionization mechanism via the reaction: $e^- + H_2 \rightarrow 2e^- + H_2^+$. The electron density increases with pressure. The current measured by the RFEA directly after the EUV pulse consists of 2 components (Fig. 4-a). The first component is measured during approximately 1 µs after the EUV pulse. This sharp and intense current peak is caused by intense EUV light, producing secondary electron emission from the RFEA collector. The second component is the ion flux on the collector when ions from the EUV-plasma reach it through the plasma sheath. The current decreases as the EUV-plasma decays. Fig. 4-b) further illustrates several time-resolved ion energy distributions at pressures 1-20 Pa. It can be noticed that the ion energy reduces with pressure due to collisions in the sheath at higher pressures, however the ion energies do not show a big difference. The peak energies stay in the range of 2-6 eV, so that the difference is insignificant: 6 eV at 1-2 Pa and 2 eV at 20 Pa.

The reduction of ion energies at higher pressure would not significantly influence yields caused by physical sputtering due to a very low ion energy. This suggests that only chemical sputtering effects would play a role in this pressure range. The ion flux, however, increases with the pressure increase from 1 to 20 Pa (Fig. 5).

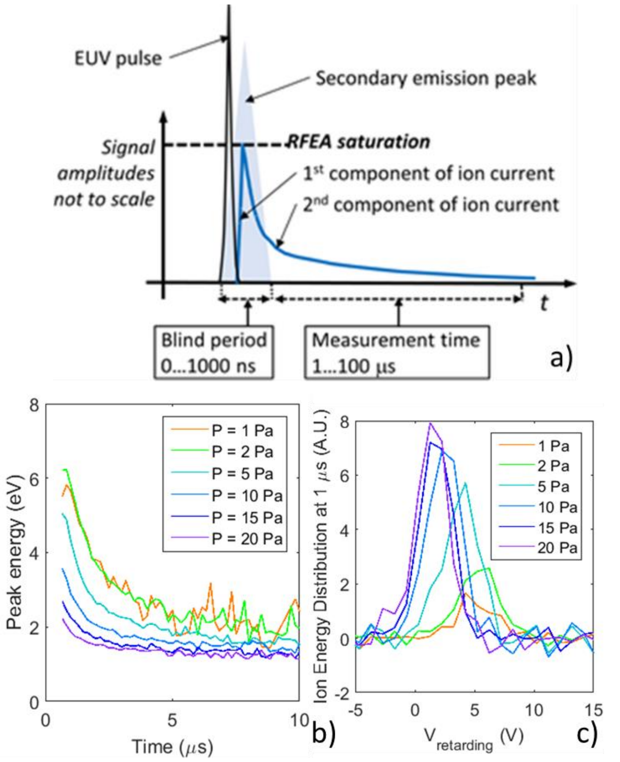

Fig. 4. a) Qualitative illustration of two ion current components measured by RFEA after the EUV pulse; b) a family of peak ion energies at pressures 1-20 Pa as a function of time after the EUV pulse and c) measured ion energy distributions at 1 µs after the EUV pulse at a position beside the EUV beam at 120 mm defocus for the range of pressures 1-20 Pa.

Therefore, a pressure increase to 10-20 Pa may be considered appropriate to accelerate materials tests.

Studies of photomasks demonstrated that the EUV intensity of a focused beam on the surface is too high, resulting in overheating of the photomask in comparison to scanner conditions. To recreate an environment more compatible with a real system, the EUV beam was defocused to decrease the power density in the center and to reduce overheating of the photomask.

On another hand, accelerated tests of the equipment demand that higher ion dose (D) is achieved within shorter time, $D = \Phi\ (\mathrm{ions}\cdot\mathrm{m}^{-2}\mathrm{s}^{-1})\cdot A(\mathrm{m}^2)\cdot(\mathrm{time})$. In the case of a defocused beam, lower ion fluxes are produced, however, the ion flux can be restored by using higher pressures. Also, a larger sampling area can be utilized for photomask exposures in the defocused case. This opportunity is summarized in Fig. 5-a). Lines 1-2 show ion fluxes as functions of pressure for a defocused beam at distances of 0 and 17 mm from the center of the EUV beam, as it is schematically illustrated in Inset 1. Inset 2 shows the case, when the beam is focused at the distance of 8 mm. The ion flux could not be measured in the center due to a too high EUV intensity, leading to possible sensor damage. Clearly in the defocused case, the ion flux is only slightly lower at 17 mm than the ion flux at 8 mm in the focused case, even at higher pressures.

Space-resolved ion fluxes are depicted in Fig. 5 b) for various pressures and for various defocus settings of the EUV beam. The insets illustrate the settings for the various measurements. When comparing line 1 with line 2 and line 4 with line 5, it can clearly be seen that increasing the pressure results in higher ion fluxes in a larger area. At low pressures and large defocus settings of the EUV beam (lines 1 and 2), the beam shapes are still relatively uniform. With larger pressure differences and with a focused EUV beam (lines 4 and 5) it becomes clear that the beam shape changes, becoming sharper for higher pressures due to a larger number of collisions.

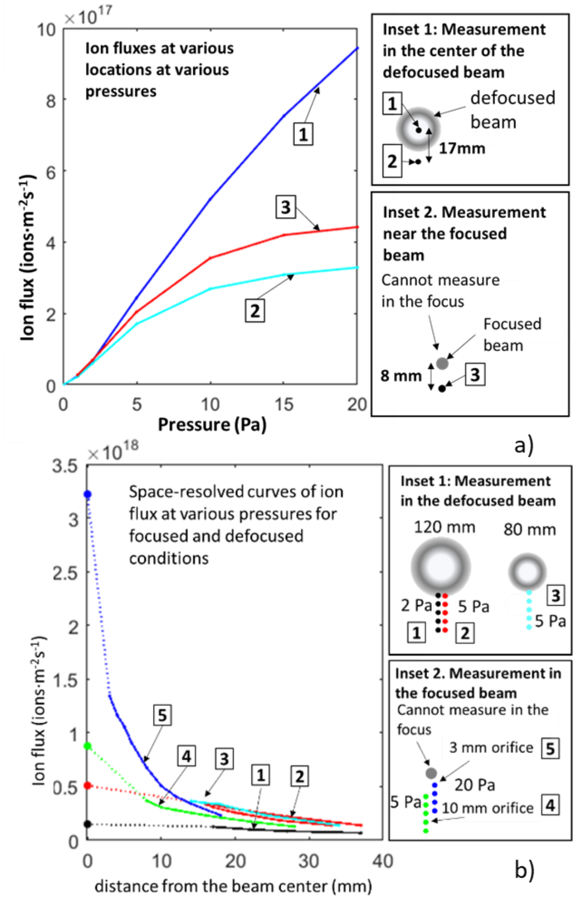

Fig. 5. a) ion fluxes measured in an EUV-induced plasma as a function of pressure for different beam conditions. Inset 1-2 show measurements positions with respect to the beam center; b) ion fluxes measured as functions of the distance from the beam center, for focused and defocused EUV beams at pressures 2, 5 and 20 Pa. Insets 1-2 show the measurement positions with respect to the beam center.

4. Photomask measurements

Considering plasma interactions with photomasks, in general, several effects can be mentioned such as: carbon reduction, oxygen and oxides reduction and overall contamination reduction. For instance, it has been found in the earlier work [4], that fluorine contamination was reduced at areas with higher ion flux. Mechanisms explaining the reduction of fluorine may include a photolysis of surface fluorine radicals in the EUV beam and their interaction with plasma species (such as for example: $CF_x + h\nu \;/\; e^- \rightarrow \; CF_{x-1} + F + e^-$), similar to the VUV-enabled halogen radicals desorption from polymer films. Chemical interaction of ions and radicals with the surface-bonded fluorine can also be suggested [13-14].

A reduction of C and decrease of O can be considered for the Ru-based photomask capping layer as the data of Table 2 illustrates for the defocused EUV beam. Here, "Pre-exp" stands for the XPS measurements before the exposure; "0 mm" and "30 mm" – for the XPS measurements after the exposure at 0 and 30 mm from the beam center. The key elements present in the XPS analysis are normalized without C. No difference between Ru-samples placed in the center of the EUV beam and at 30 mm from the center can be noticed. This may mean that the exposure duration was sufficiently long to reach the needed effects both in the center and at the periphery of the plasma.

For other dose-dependent effects, which may require higher doses with higher fluxes within the limited time, it may be proposed to use higher pressures as the measurements at 2 and 5 Pa show insignificant difference.

Table 2. Summary of XPS characterization showing key elements of Ru-based photomask [at.%], normalized to 100% without C

Samples	Mo 3d	O 1s	Ru 3d	Si 2p	C 1s
Exposed to EUV induced plasma at 2 Pa					
Pre-exp	1.1	40.6	38.9	19.4	36.9
0 mm	1.6	15.7	57.4	25.2	22.6
30 mm	1.7	11.9	60.0	26.4	21.0
Exposed to EUV induced plasma at 5 Pa					
Pre-exp	1.0	41.2	38.5	19.3	29.9
0 mm	1.5	15.6	56.7	26.2	23.4
30 mm	1.5	14.6	57.3	26.6	23.4

5. Summary

Hydrogen low-density plasmas induced with a defocused EUV-beam were studied, and ion fluxes in the range of (2-8)·10^{16} ions·$m^{-2}s^{-1}$ were measured. Space- and pressure-resolved ion fluxes were produced in the EBL-2 research facility on photomask surfaces and modifications of Ru photomasks were analyzed. For Ru-layers, reduction of C and O was observed. Higher pressures might accelerate tests as ion fluxes increase 3-4 times at 20 Pa and required doses may be achieved faster. Measured ion energies did not vary significantly with pressure (2-6 eV), making physical sputtering negligible.

6. References

[1] J. Beckers et al., Appl. Sci. 9, 2827 (2019).
[2] M. van de Kerkhof, et al., Radiation Effects and Defects in Solids 177:5-6, 486-512 (2022).
[3] M. van de Kerkhof, et al., J. Micro/Nanopatterning, Materials, Metrol. 20, 033801 (2021).
[4] J. van Veldhoven et al., J. Vac. Sci. Technol. B (2023).
[5] T.H.M Van De Ven, et al., J. Appl. Phys. 123, 063301 (2018).
[6] D.C. Brandt, et al., Proc. SPIE 9048, 90480C (2014).
[7] J. van Veldhoven et al., IEEE Trans. Plasma Sci. 49, 3132 (2021).
[8] E. te Sligte, et al., Proc. SPIE 9984, 99840R (2016).
[9] E. te Sligte, et al., Proc. SPIE 9985, 998520 (2016).
[10] H. Bekman, et al., Proc. SPIE 11147, 1114706 (2019).
[11] D. Ugur et al., Microelectronic Engineering 110, 60-65 (2013).
[12] J. Velthuis et al., J. Vacuum Sci. Technol. A 37, 061302 (2019).
[13] A. Vesel, et al., Appl. Surf. Sci. 357, 1325 (2015).
[14] V. Skurat, Nucl. Instr. and Meth. in Phys. Res. B 208, 27 (2003).